Int. Journal of Refractory Metals and Hard Materials 29 (2011) 188–201

Contents lists available at ScienceDirect

Int. Journal of Refractory Metals and Hard Materials

journal homepage: www.elsevier.com/locate/IJRMHM

The effect of consolidation parameters on the mechanical properties of binderless tungsten carbide

Kuo-Ming Tsai *

Department of Mechanical Engineering, National Chin-Yi University of Technology, No. 35, LN 215, SEC 1, Chung Shan RD, Tai-Ping, Taichung 411, Taiwan, ROC

ARTICLE INFO

Article history:
Received 30 August 2010
Accepted 26 October 2010

Keywords:
Binderless tungsten carbide
Ball-mill
Particle-size analysis
Sintered density
Mechanical properties

ABSTRACT

This paper discusses the effect of the process parameters on the mechanical properties of binderless pure tungsten carbide during a GPS (gas protection sintering) process. The result of experiments reveal that the mechanical properties of the material increases with raising the sintering temperature and extending the retention time; however a decreased hardness was observed as a result of abnormal grain growth under higher sintering temperatures. The results of XRD and EDS analyses confirmed the absence of brittle phases such as W_2C or impurity phases in the microstructure. The optimized process parameters for GPS process are identified as: a mean particle size of 1.03 μm, a sintering temperature of 1860 °C and a retention time of 60 min; the resulting mechanical properties are: a relative density of 95.1%, a micro-hardness of 1718 kgf/mm^2 and a fracture toughness of 5.97 MPa m$^{1/2}$. The width of particles size distribution has a significant effect on the density and hardness of the sintered material however the width of particles size distribution is dependent on the original particle size. Finally, ultra-fine particles increase the chance of conglomeration and sub-micron structures. The conglomeration of ultra-fine particles hinders the filling of porosities during sintering and lowers the density and hardness of the material.

1. Introduction

Cobalt bonded tungsten carbide, WC, is a high performance tool material with high hardness, high abrasive resistance, low coefficient of friction and excellent dimensional stability; they are widely used for cutting tools, dies, moulds and other abrasion resistant products. The fundamental role of the binder phase, Co, is to assist complete densification of the material however the presence of a cobalt binder deteriorates hardness, corrosion resistance and oxidation resistance of the material [1]. The discrepancy in the thermal expansion coefficients of WC ($2.0\times10^6\,K^{-1}$) and Co ($13.8\times10^6\,K^{-1}$) incurs thermal stress in the material. Compared with the pure WC phase, a Co binder is prone to corrosion and oxidation in the presence of harsh chemicals consequently cobalt bonded tungsten carbides are not applicable for these environmental conditions. However these problems can be relieved by decreasing Co concentration in the material.

Binderless pure tungsten carbide refers to hardmetals containing little or no metallic binder [2]. Binderless pure tungsten carbide is sintered without metallic binders such as Co, Fe or Ni. The material shows a higher resistance to abrasion, corrosion and oxidation while its polishing characteristics are better than cobalt bonded tungsten carbide. Applications for this material includes electronic packaging, moulds and dies for optical elements [3] and high temperature corrosive resistant piping.

The processing parameters significantly affect the mechanical properties of the sintered material. Research studies revealed that the hardness and densification of the product increase with decreasing particle diameter and that complete densification has not been attained because of conglomeration of the initial powder as well as surface oxidation and contaminations of samples [4,5]. The sintering temperature for tungsten carbide with 3% to 20% cobalt binder is 1370–1490 °C, whereas for binderless pure tungsten carbide the required temperature is 1800–2000 °C [6]. Generally, excessively long retention time or high sintering temperature incurs porosities in the material and leads to coarsening of the microstructure. Therefore the proper control of sintering time and temperature during the process is crucial for producing materials with superior mechanical properties; insufficient or excess retention time at high temperature is detrimental to the mechanical properties [4]. At higher temperatures, the pure tungsten carbide particles are bonded together through diffusion mechanism and hence increase the material strength however excess retention time induces grain growth that deteriorates the strength of the material [7]. This study investigates the effect of parameters such as particle size, sintering temperature and retention time in the GPS process and their resultant outcomes on the density, hardness and fracture toughness of the binderless pure tungsten carbide.

* Tel.: +886 423924505x7175; fax: +886 423930681.
E-mail address: tsai101@ncut.edu.tw.

0263-4368/$ – see front matter © 2010 Elsevier Ltd. All rights reserved.
doi:10.1016/j.ijrmhm.2010.10.006

2. Experimental setup

2.1. Experimental procedures

The experimental parameters of the GPS process used in this research are listed in Table 1. The three major process parameters used for the sintering experiments are powder size, sintering temperature and retention time — with each parameter having three variations.

Fig. 1 shows the surface morphology of pure tungsten carbide particles used, a powder produced by Allegheny Technology Inc., USA. The pure tungsten carbide powder, together with Φ8 mm tungsten carbide balls and volatile n-Hexane were loaded into the ball-mill jar to implement wet horizontal ball milling. The powder was uniformly mixed with 1.5 wt.% paraffin wax in a heated water bath after the ball milling. In the milling 100 WC balls are used, each with Φ8 mm in diameter. The total weight of the balls is 400 g and the ratio of WC powder to balls weight is 0.3. The space of milling chamber is 1000 cm^3, with 600 cm^3 occupied by the WC powder and the balls. The powder was then compacted in a 10 t hydraulic press at the specified pressure with the resultant green discs of $\Phi 18.1 \times 4.7$ mm then loaded into an inert gas protected sintering furnace. The argon gas was directed into the furnace chamber after the vacuumed pressure had reached $1.0 \times 10^{-1} - 5.0 \times 10^{-2}$ Torr. The furnace was then heated to the de-waxing temperature and then the sintering temperature at the specified heating rate and retention time. The sintered samples were then grinded by 30 μm, 15 μm, 9 μm and 3 μm grit diamond grinder plates respectively, then polished using diamond polishing liquid allowing observation by a microscope.

2.2. Particle size analysis

The particle size of powder is a significant factor for the sintering process. A Laser Diffraction Particle Size Analysis System (LA-950, by Horiba ABX Inc., Japan) was used to determine the mean diameter and the distribution of particle size for the original powder as well as the 24 h ball milled pure tungsten carbide powder; the average of these two measurements were then taken as the empirical data for each specimen.

2.3. Heating procedure

The pure tungsten carbide powder was mixed with paraffin wax to facilitate pressing of powder into green disc samples for the sintering process. The amount of wax used is very critical because the wax must be uniformly and be completely evaporated during the degreasing process. A thermal gravimetric analyzer, TGA (Q500 by TA Instruments, USA), was used to determine changes in sample weight as a function of temperature; the heating rate used was 20 °C/min, up to 800 °C.

Fig. 2 shows the TGA results; the paraffin wax started to evaporate near 200 °C while the rate of evaporation increases with the rising temperature. Between 400 and 500 °C the paraffin vaporized rapidly and the evaporation process ended at 500 °C. An inadequate degreasing temperature may induce a defect or distortion of the product while an excessively high degreasing temperature can even rapidly evaporate the paraffin wax and disintegrate the parison. However, an excessively low degreasing temperature may incur retained carbide during the thermal decomposition stage of sintering process and deteriorate the ductility and strength of the material [8].

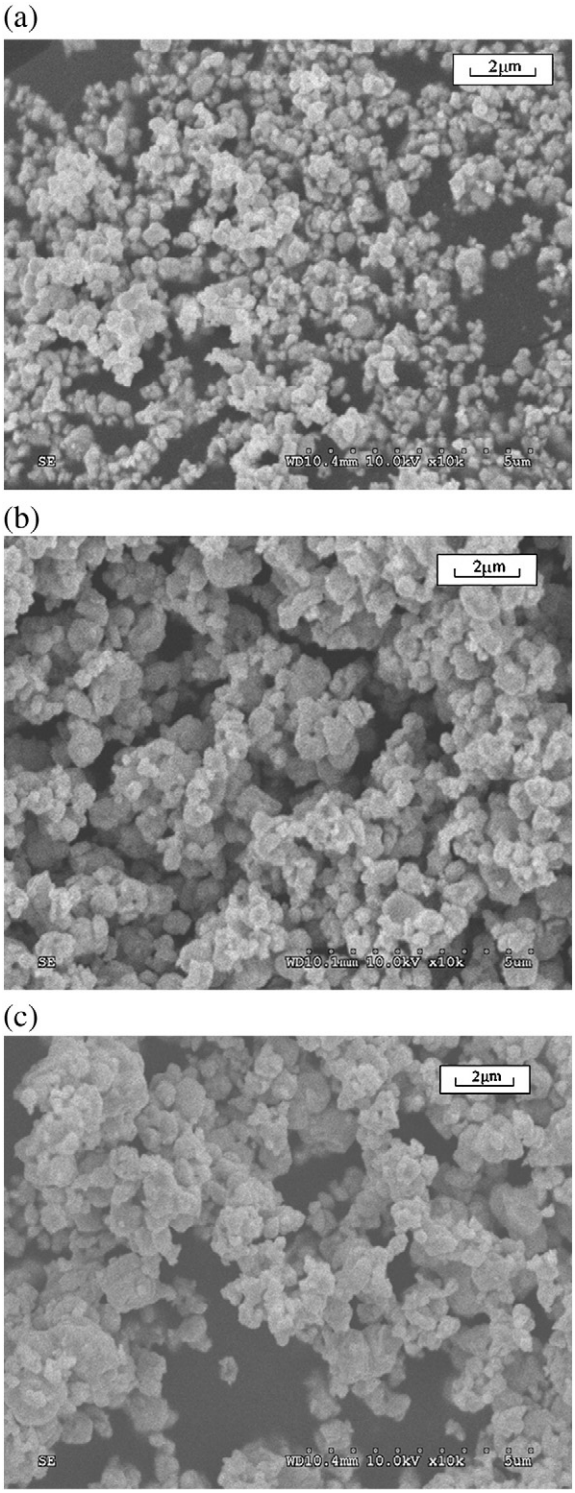

Fig. 1. SEM micrographs of the initial pure WC powders: (a) 0.66, (b) 0.87 and (c) 1.36 μm.

Table 1
Experimental parameters.

Parameters	Level		
	1	2	3
Mean powder size(μm)	0.66	0.87	1.36
Retention time(min)	0	30	60
Sinter temperature(°C)	1740	1800	1860
Ball milling time(h)	24	–	–
Pressing pressure(MPa)	250	–	–
Argon flow rate(cc/min)	15–20	–	–

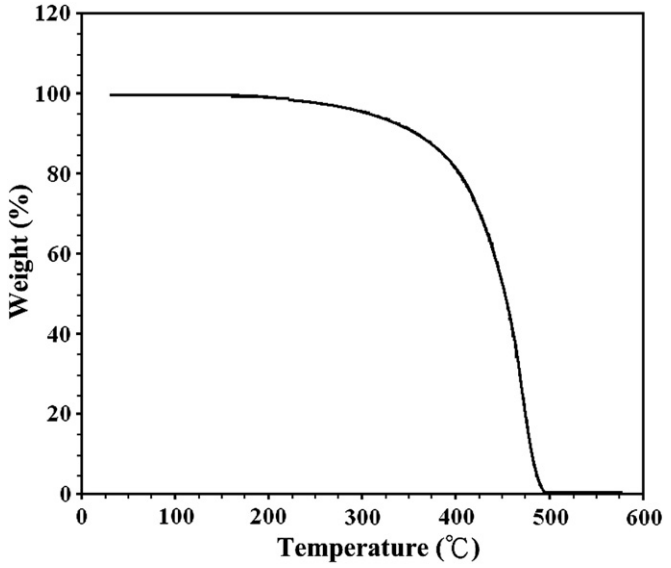

Fig. 2. Weight loss curve of paraffin wax. The paraffin wax started to evaporate near 200 °C while the rate of evaporation increases with the rising temperature.

The TGA curve obtained was used to determine the degreasing time and temperature resulting in an identification of the temperature for each stage of the sintering process. From these findings an extended retention time at 300 °C was used because the paraffin evaporates slower at 200–300 °C while the other retention temperatures were chosen as 420 °C and 500 °C because the paraffin evaporates quickly between 400 °C and 500 °C.

Fig. 3 shows the heating profile for the sintering process. The process below 520 °C was the degreasing stage in which a low heating rate of 3 °C/min was used to allow complete evaporation of paraffin within the parison. After the degreasing stage the heating rate was increased to 6 °C/min, up to 1500 °C. The heating rate for the final stage of sintering was 3 °C/min, up to the sintering temperature, and therefore allowed the diffusion bonding at the interface of particles to occur.

2.4. Density and hardness measurements

The densities of the sintered samples were measured in compliance with to ASTM Standard B328-94 based on the Archimedes' principle. A Vickers micro-hardness tester (FV-300e by Nakazawa Co., Japan) was used to measure the micro-hardness of the samples; a standard micro-Vickers indenter was used to apply a 9.8 N load on each sample for 15 s. The distance from the center of the indentation to the end of the crack tip was measured to determine the fracture toughness, K_{IC}, of the material; the equation used to calculate K_{IC} is shown in Eq. (1) [9].

$$K_{IC} = 0.016\left[\frac{E}{Hv}\right]^{1/2}\cdot\frac{P}{C^{3/2}} \quad (1)$$

where E is the Young's Modulus of 550 GPa for binderless tungsten carbide, Hv is the Vickers micro-hardness of the material, P is the indentation load (gf) and C is the distance (μm) from the center of indentation to the crack tip. As is apparent from the equation, K_{IC} of the material is intimately related to the length of the crack, materials with high K_{IC} tend to be more resistant to crack propagation.

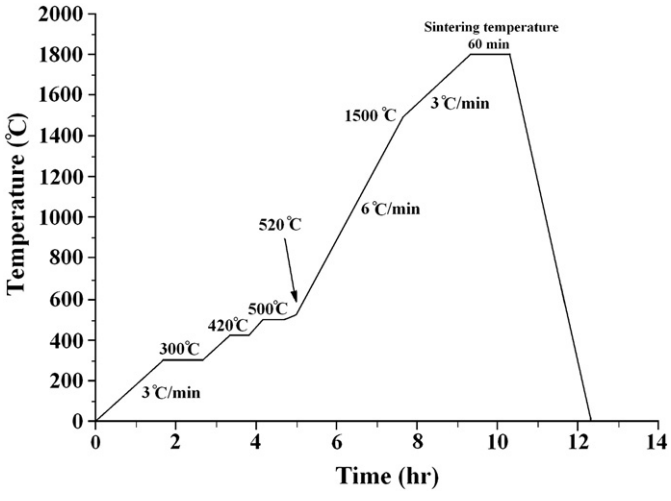

Fig. 3. Heating route for the sintering process. There are three stages using different heating rate in the process.

2.5. Phase structure and microstructure analysis

The tungsten carbide samples were analyzed in an X-ray diffractometer, XRD, (Rigaku D/Max 2200/PC) with Cu-K_α radiation ($\lambda = 1.5417$ Å) at 40 kV and 40 mA to determine the crystal structure, grain size and the lattice constant of the material. The scan rate was 0.02°/s in the scattering angular range (2θ) of 20 to 80°. The grain morphology and the microstructure of the samples were observed in a high resolution Variable Vacuum Scanning Electron Microscope, VV-SEM, (S3000 by Hitachi Co., Japan), operated at 10 kV. The Energy Dispersive Spectroscopy, EDS, at the VV-SEM was used to identify the constituents of each phase in the material. Optical micrographs were also taken as a comparison with the SEM micrographs.

3. Result and discussion

3.1. Particle size analysis

This paper investigates mechanical properties of binderless pure tungsten carbide products sintered from powders of different particle size by using a GPS process. Fig. 4 shows the results of Laser diffraction particle size analysis for the pure tungsten carbide powders with three different particle sizes before and after 24 h ball-mill. The result indicates that for all the three types of powders the particle sizes are smaller after ball milling for 24 h. The reason for this is that the particles are grinded and impacted among the tungsten carbide balls and between the wall of milling jar and the balls. After ball milling the particle sizes of the powders are smaller and the distributions of particle size are narrower. When the mean particle size of WC decreases the width of distribution also decreases, therefore the intensity is higher near the mean and the distribution becomes narrower. The reason is that, for the ball-size used, the refining process slows down when the particles reach a certain diameter (near 0.6 μm), and the remaining larger particles continue to be refined with extended milling time. Fig. 5 shows the change in particle size distribution after 24 h of ball milling using Φ8 mm diameter tungsten carbide balls. For the 1.03 μm powder, particles with diameter larger than 1.5 μm are refined to about 1 μm. This suggests that for the Φ8 mm ball used the tungsten carbide particles can only be grinded to 1 μm in diameter; the particles cannot be refined to diameters much smaller than 1 μm after 24 h of milling using Φ8 mm balls. Similar results are obtained for 0.63 μm and 0.84 μm powders; particles larger than 1 μm are refined to about 1 μm in diameter.

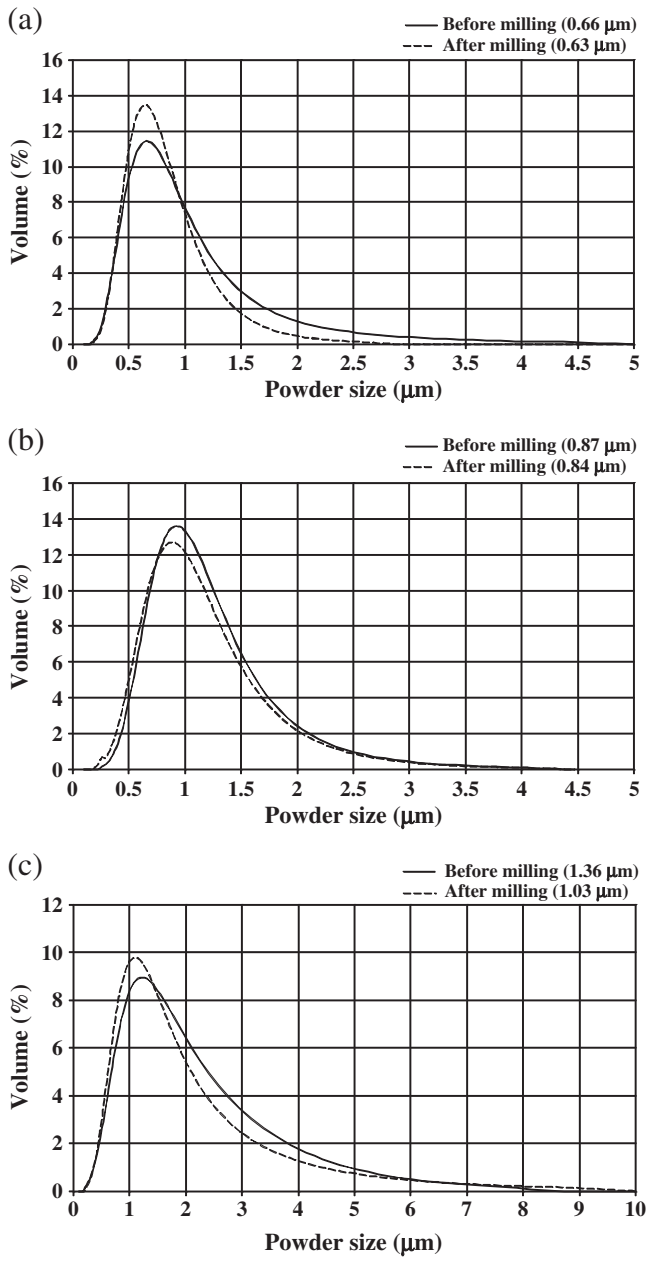

Fig. 4. Particle size distributions of the powders after ball milling process: (a) 0.66, (b) 0.87 and (c) 1.36 μm. After ball milling the mean particle sizes of the powders are smaller and the distributions of particle size are narrower.

3.2. Phase structure

Tungsten carbides with de-carbonated W_2C or other impurity phases are more brittle and with less hardness [10,11]. Fig. 6 shows the XRD patterns for the original powders and the sintered specimens; the substrate phase is pure WC only, without W_2C or other impurity phases. Fig. 7 shows the EDS data for specimens made from different sized powders; the only phase present is WC which is in agreement with the XRD results.

3.3. Density

The density of the material is closely related to the temperatures and retention time of the sintering process. The relative density of the sintered specimens as a percentage compared with the theoretical

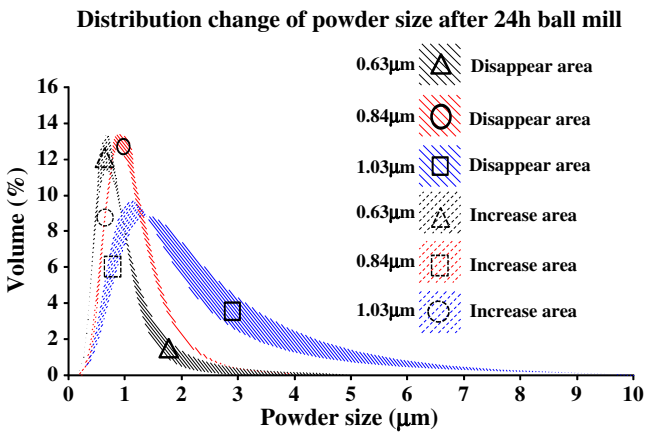

Fig. 5. Particle-size distribution changes of three powders after 24 h ball milling.

value of 15.53 g/cm^3. Fig. 8 shows the effect of the sintering temperature on the density of the material. The distance of mass transportation increases with the increasing diffusivity of the material which increases exponentially with the process temperature, therefore diffusion bondings at the particle boundaries and other high diffusivity paths are enhanced at higher temperatures. At high temperatures, reorientation of WC particles occurs and pores are filled as a result of boundary sliding and grain rotation, resulting in higher density materials [12]. The effect of the retention time on the density of the material is shown in Fig. 9. The result of the experiment indicates that the density of the material increases with increasing the retention time while the distance of diffusion also increases with lengthening the retention time. Therefore a prolonged retention time enhances diffusion within the grains; however excessive retention time results in grain coarsening which deteriorates the mechanical properties of the material.

3.4. Microstructure

In this study a high resolution VV-SEM was used to observe the microstructure of the sintered samples. Fig. 10 shows the SEM micrographs for the 1.03 μm specimens with a 60 min retention time under different sintering temperatures. For specimens with a 1740 °C sintering temperature a porous structure of open porosities at the structure and the original spherical particles were observed via a micrograph. The porosity in the material is less severe for specimens sintered at 1800 °C; most of the pores are filled and cohesive necks are formed as a result of diffusion. At higher temperature, neck growths rapidly are observed in specimens with a sintering temperature of 1860 °C; intergranular pores are coalesced to form closed pores. Particles of different sizes are conglomerated to form coarse grains while heterogeneous distributions of spherical grains are still present. Fig. 11 shows the SEM micrographs for the 1.03 μm specimens under a sintering temperature of 1860 °C with different retention times. The figure reveals that for specimens sintered at 1860 °C without retention time, a porous structure with finer grains are obtained. With a 30 min retention at 1860 °C, less fine grains are observed and the porosities are decreased; the densification of the material was enhanced as a result of the high diffusivity at the retention temperature. Significant grain growth was observed for specimens with a 60 min of retention at 1860 °C; the severe intergranular conglomeration produces coarsened grains which deteriorated the mechanical properties of the material. Fig. 12 shows the SEM micrographs for specimens made from different sizes of powders under a sintering temperature of 1860 °C and with a 60 min retention. For specimens made from 0.63 μm powder, the grain size is smaller

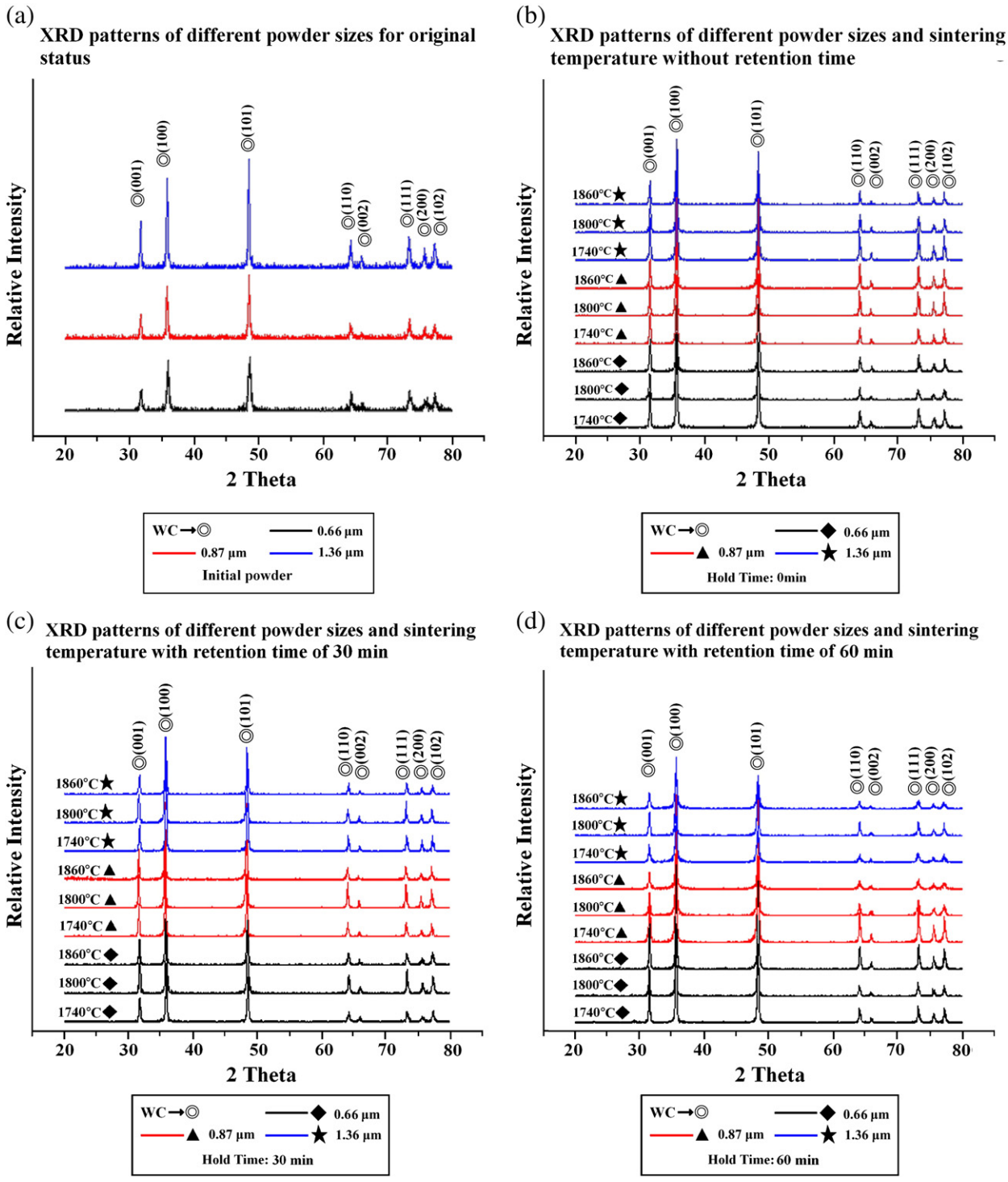

Fig. 6. XRD patterns of initial powders and sintered specimens: (a) Initial powder, (b) Without retention time, (c) 30 min retention and (d) 60 min retention. The phase of all substrates is pure WC only.

and the density is lower because of the enclosed pores within the coalesced particles at the early stage of the sintering process hampering the filling of intergranular pores.

3.5. Mechanical properties

This section discusses the effect of sintering temperature and retention time on the hardness and fracture toughness of the material.

3.5.1. Micro-hardness

The effect of sintering temperature on the micro-hardness of the material is shown in Fig. 13; the result indicates that the Vickers micro-hardness of specimens increases with the increasing temperature. The samples with a sintering temperature lower than 1740 °C have lower micro-hardness because of the presence of porosities at the microstructure; for samples sintered at 1860 °C, the micro-hardness is higher because of the low porosity in the material. Fig. 14 shows the micro-hardness for specimens made

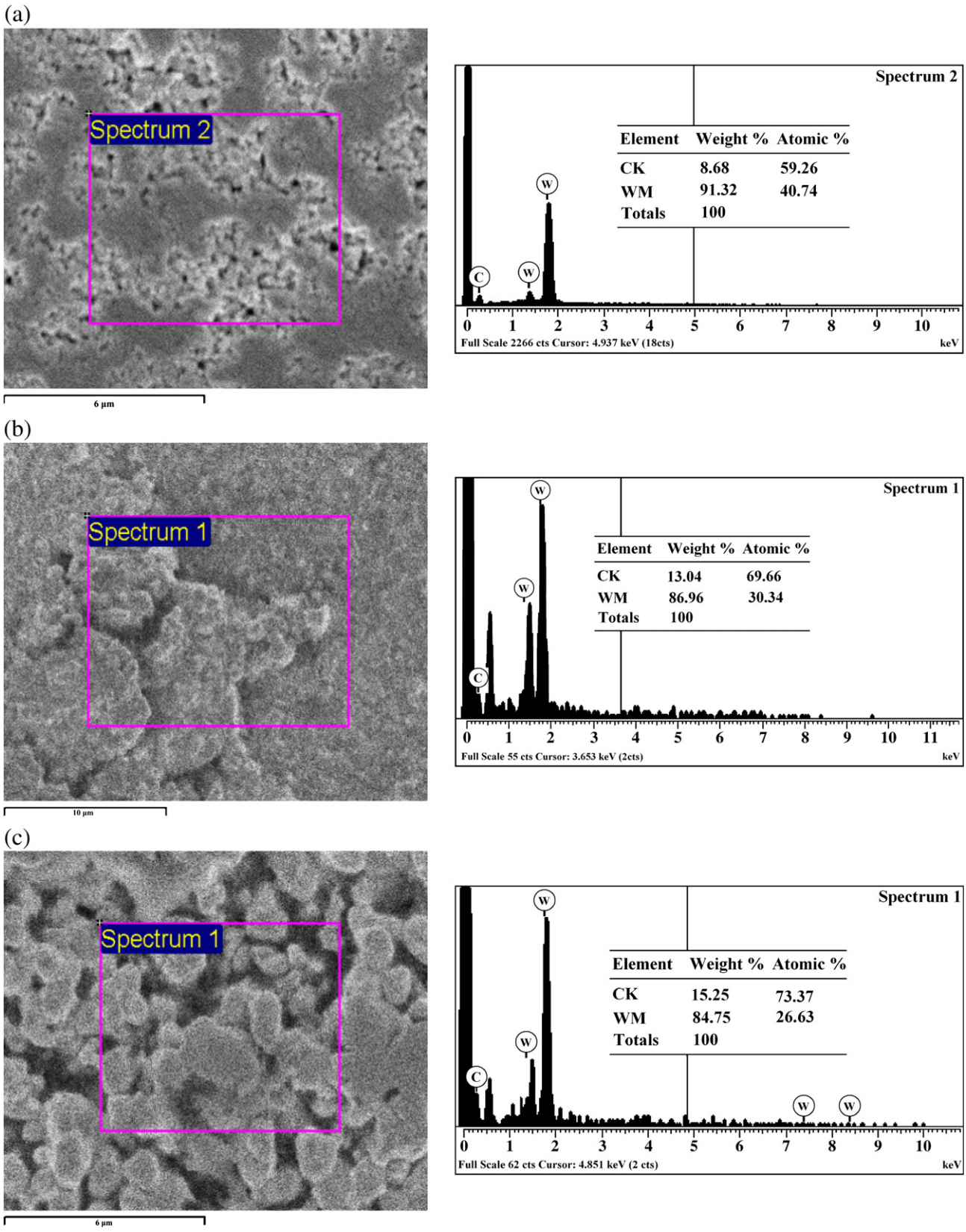

Fig. 7. EDS data of specimens made from initial powders (sintering temperature: 1860 °C, Retention time: 60 min): (a) 0.66, (b) 0.87 and (c) 1.36 μm. The only phase present is WC which is in agreement with the XRD results.

from differently sized powders and sintered at different temperatures with different retention times. Theoretically, increasing the retention time is beneficial for homogenization of the microstructure of materials, except for over-sintering. However, at the stage of sintering where pores are coalesced into spherical pores, the increase in the retention time may deteriorate the mechanical

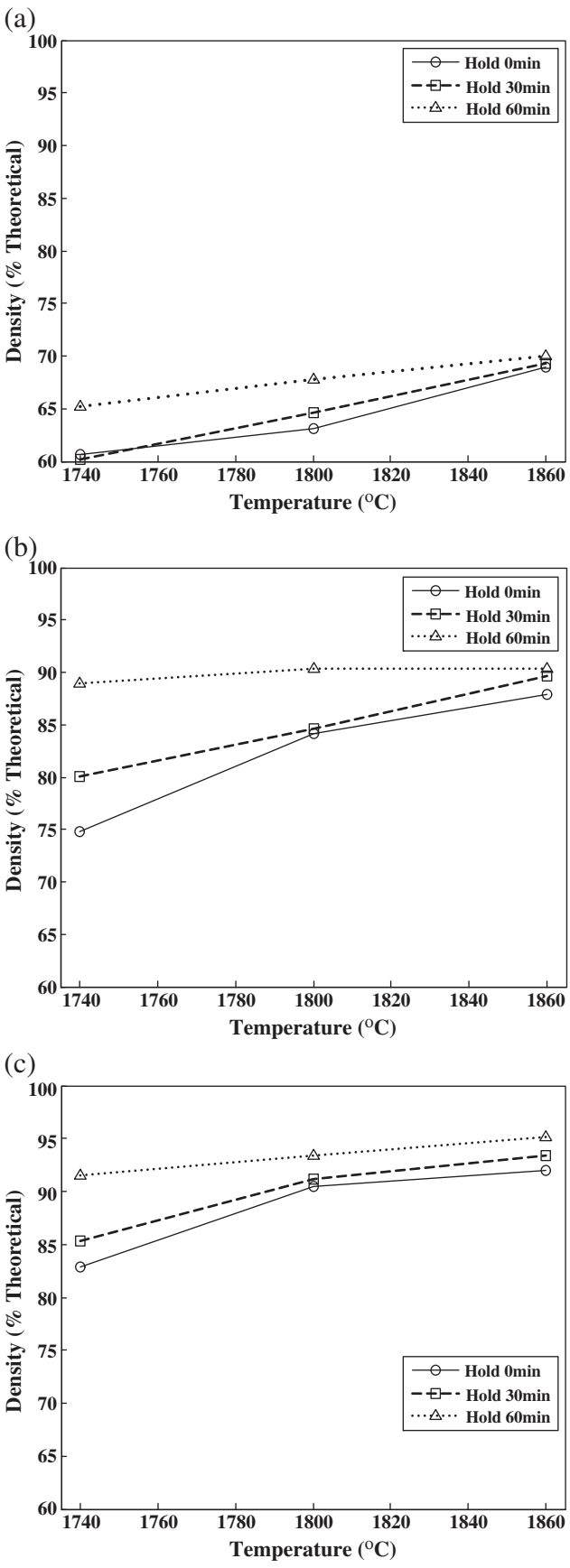

Fig. 8. Relative densities of specimens at different mean powder sizes and sintering temperatures: (a) 0.63, (b) 0.84 and (c) 1.03 μm. The diffusion bondings among the particles are enhanced at higher temperatures.

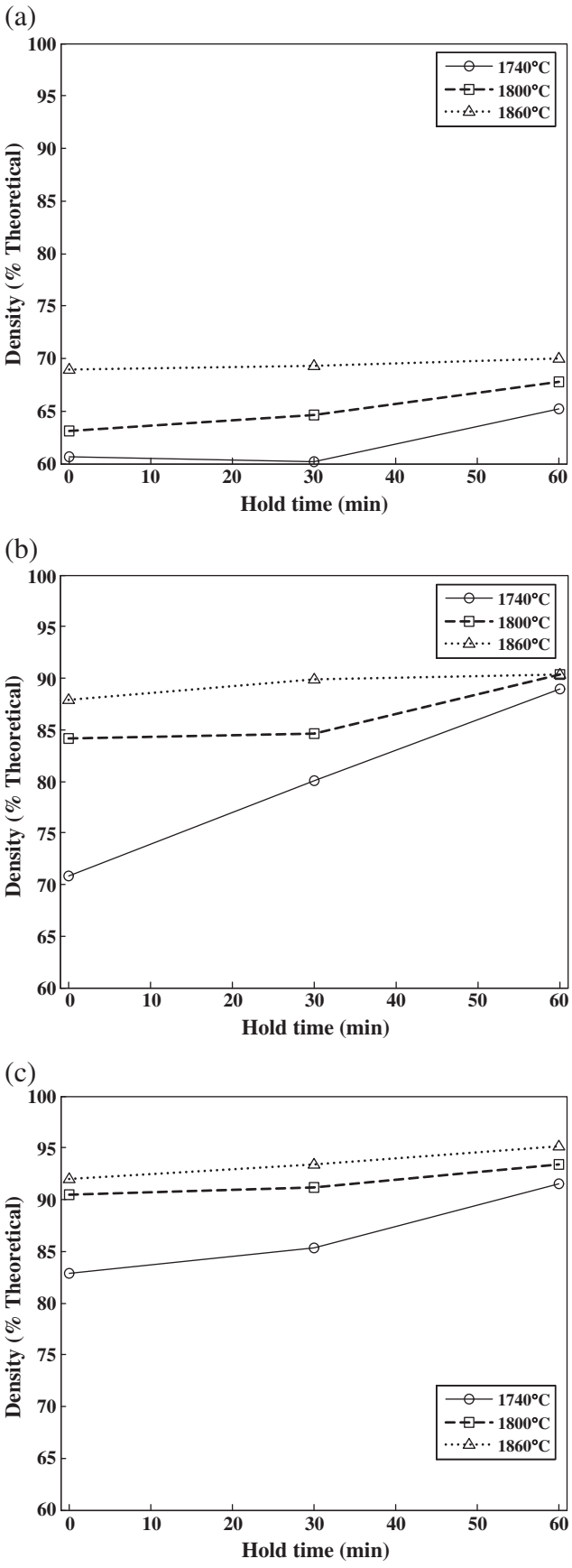

Fig. 9. Relative densities of specimens at different mean powder sizes and retention times: (a) 0.63, (b) 0.84 and (c) 1.03 μm. The result indicates that a prolonged retention time enhances the diffusion among the particles.

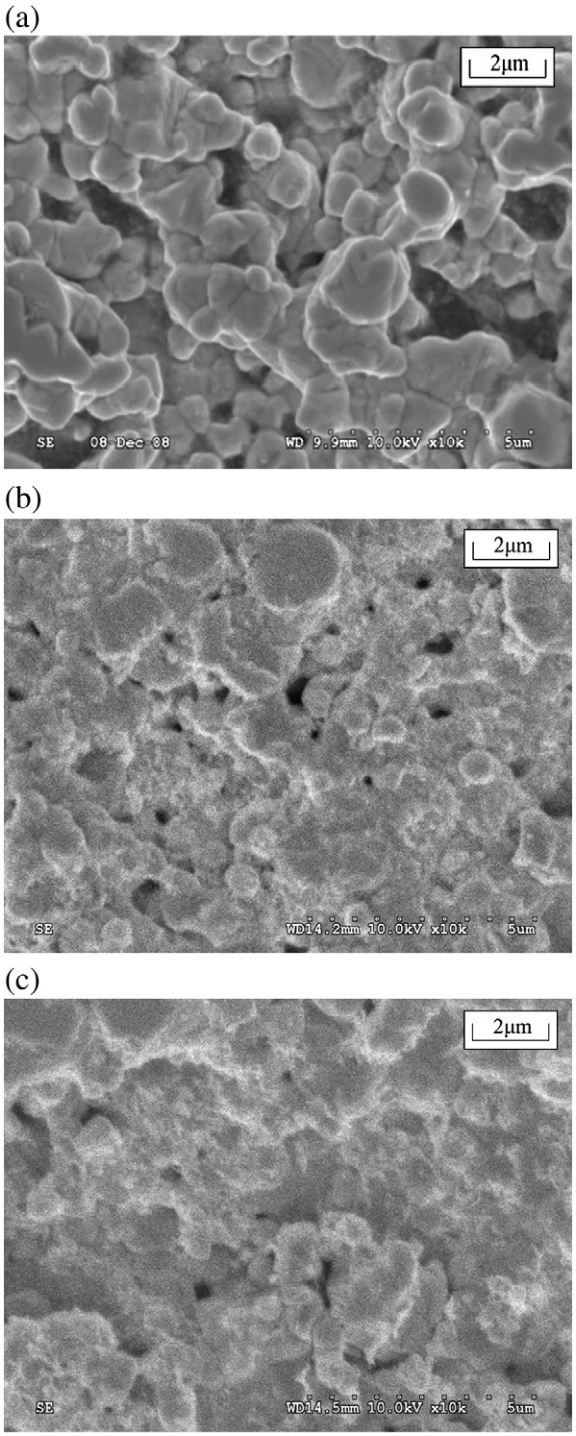

Fig. 10. SEM micrographs of 1.03 μm particle specimens at different sintering temperature with 60 min retention: (a) 1740, (b) 1800 and (c) 1860 °C. Intergranular pores decrease with the increasing sintering temperature.

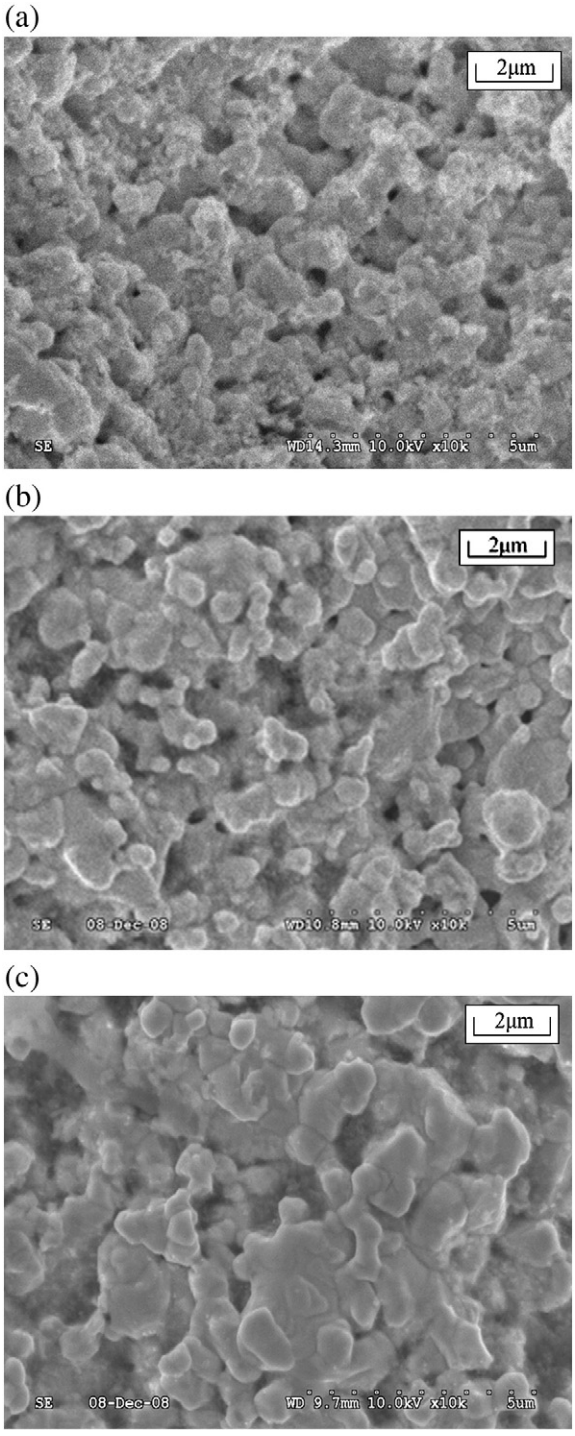

Fig. 11. SEM micrographs of 1.03 μm particle specimens at a sintering temperature of 1860 °C with different retention time: (a) Without retention time, (b) 30 min and (c) 60 min. Intergranular pores decrease with the increasing retention time.

properties of the material [13]. The result of the experiments reveals that the hardness of the material increases with the increasing of the retention time.

3.5.2. Fracture toughness

Vickers indentation test is widely used to evaluate the fracture toughness of brittle materials because the polished area required is small. Fig. 15 shows the Vickers indentation micrograph for a specimen made from a 1.03 μm powder sintered at 1860 °C with a 60 min retention; from each corner of the indentation a crack-tip propagates to form the crack paths. The length of cracks from the center of indentation to the crack tip is used to calculate K_{IC} using Eq. (1) with the result was shown in Fig. 16. For the 0.63 μm specimens the fracture toughness cannot be determined because of the porous surface and the irregular indentation pit. The fracture toughness for the conventional tungsten carbide depends on the quantity and distribution of the metallic binder; for binderless pure tungsten carbide, the fracture toughness depends on the grain size of

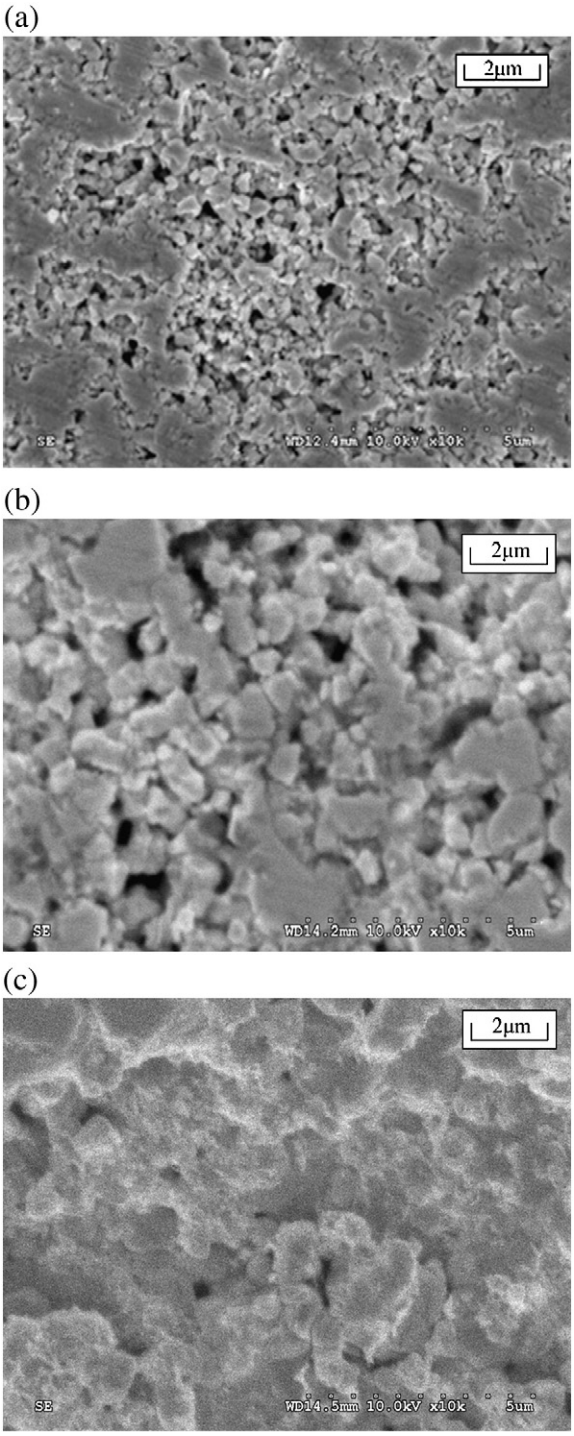

Fig. 12. SEM micrographs of specimens made from different mean sized powders under a sintering temperature of 1860 °C and 60 min retention: (a) 0.63, (b) 0.84 and (c) 1.03 μm. The relative density of 0.63 μm is lower because of the enclosed pores within the coalesced particles at the early stage of the sintering process hampering the filling of intergranular pores.

the material. Fig. 16(a) shows the effect of sintering temperature on the fracture toughness of the material; as the micro-hardness increases and the fracture toughness decreases with the increasing temperature. Fig. 16(b) shows the effect of retention time on the fracture toughness of the material; as the fracture toughness increases and the micro-hardness decreases with increasing temperature, as a consequence of the excessive grain growth as a result of the longer retention time at high temperatures [14].

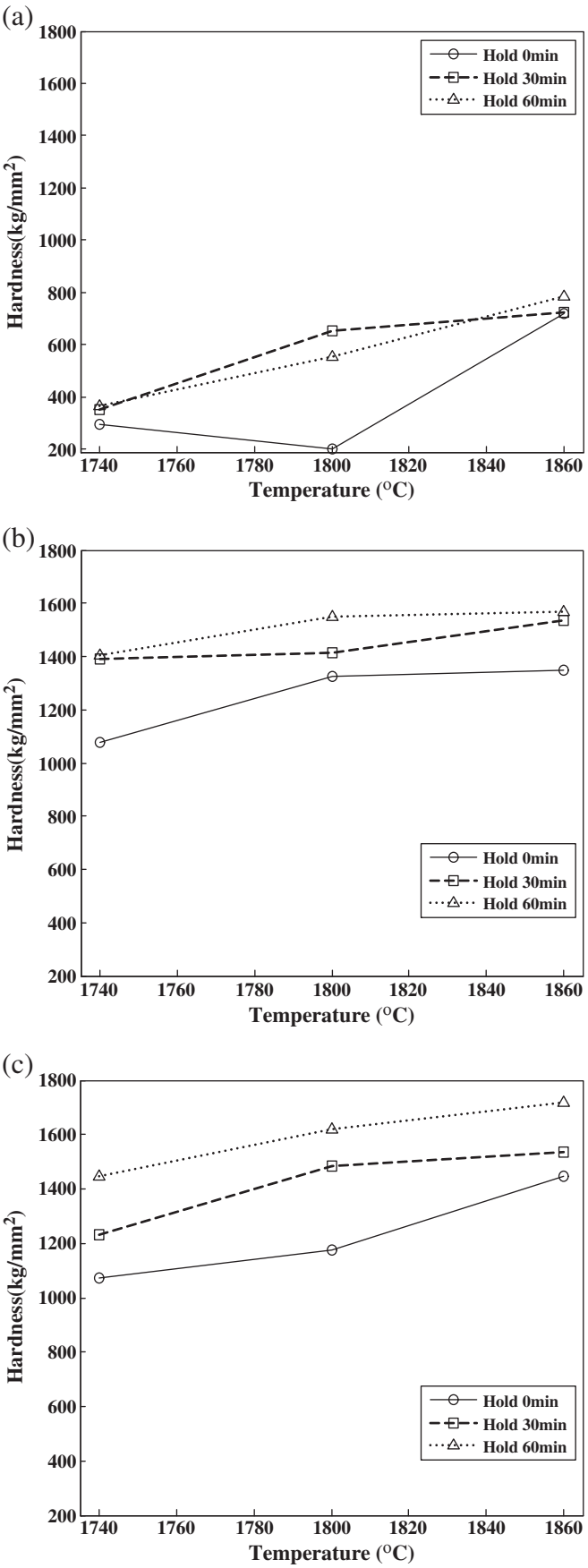

Fig. 13. Micro-hardness of specimens made from different mean sized powders and produced at different sintering temperatures: (a) 0.63, (b) 0.84 and (c) 1.03 μm. The micro-hardness of specimens increases with the increasing sintering temperature.

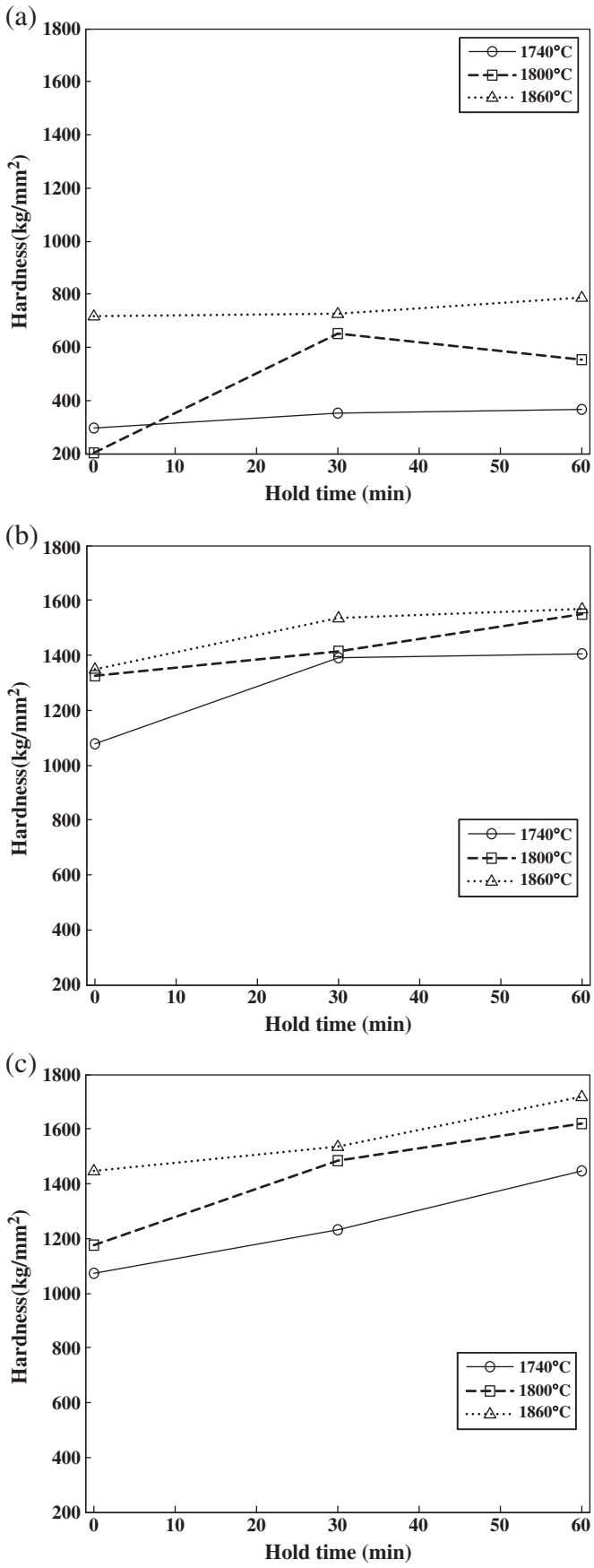

Fig. 14. Micro-hardness of specimens made from different mean sized powders and sintered at different temperatures with different retention time: (a) 0.63, (b) 0.84 and (c) 1.03 μm. Increasing the retention time is beneficial for homogenization of the microstructure of materials, except for over-sintering.

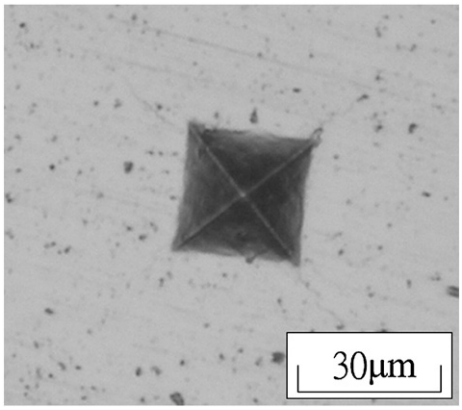

Fig. 15. Indentation in a Vickers micro-hardness test. From each corner of the indentation a crack-tip propagates to form the crack paths.

3.5.3. Surface morphology

The surface morphology of the sintered specimens was observed in an optical microscope. Fig. 17 shows the surface morphology for samples made from a 1.03 μm powder with a 60 min retention at different sintering temperatures; as the porosity decreases and the relative density and micro-hardness increases with the increasing temperature. Fig. 18 shows the surface morphology for the samples made from a 0.84 μm powder at a sintering temperature of 1860 °C with different retention times; as the porosity decreases and the density and micro-hardness increases with the increasing retention time. Fig. 19 shows the surface morphology for samples made from WC powders with different mean particle sizes at a sintering temperature of 1860 °C with a 60 min retention. In Fig. 19(a) large amount of pores are formed on the specimens made from of a 0.63 μm powder because of the trapped air within the specimens which cannot be eliminated or filled.

3.6. The effect of ball milling

Samples made from different sized powders, before and after ball milling, are studied to identify the effect of ball milling on the properties of the GPS sintered tungsten carbide. Fig. 20 shows the particle size distribution for powders after 24 h of ball milling; the particle size distribution is the widest for 1.03 μm powder and the narrowest for 0.63 μm powder. For powders with a wider particle size distribution the interstitial sites of the larger particles can be filled by fine particles; the porosities will be filled as a result of the diffusion and coalescence of the interstitial particles, producing higher density specimens. For powders with narrow distribution the volume of fine particles is not large enough to fill all the interstitial sites of the larger particles; therefore closed pores are formed at these interstitial sites, producing lower density materials. The width of particle size distribution, from wide to narrow resides in the mean powder size of 1.03 μm, followed by 0.84 μm and 0.63 μm powders. The trend in micro-hardness and density of the material closely agrees with the width of the particle size distribution; powders with a wider distribution produce harder and denser samples.

3.7. Conglomeration of ultra-fine powder

When the particle size of power is less than 0.5 μm the distance between particles is so small that the *van der Walls'* force is greater than the gravity [15]; the surface energy is larger than the volume energy of the particles, and the chance of conglomeration of the

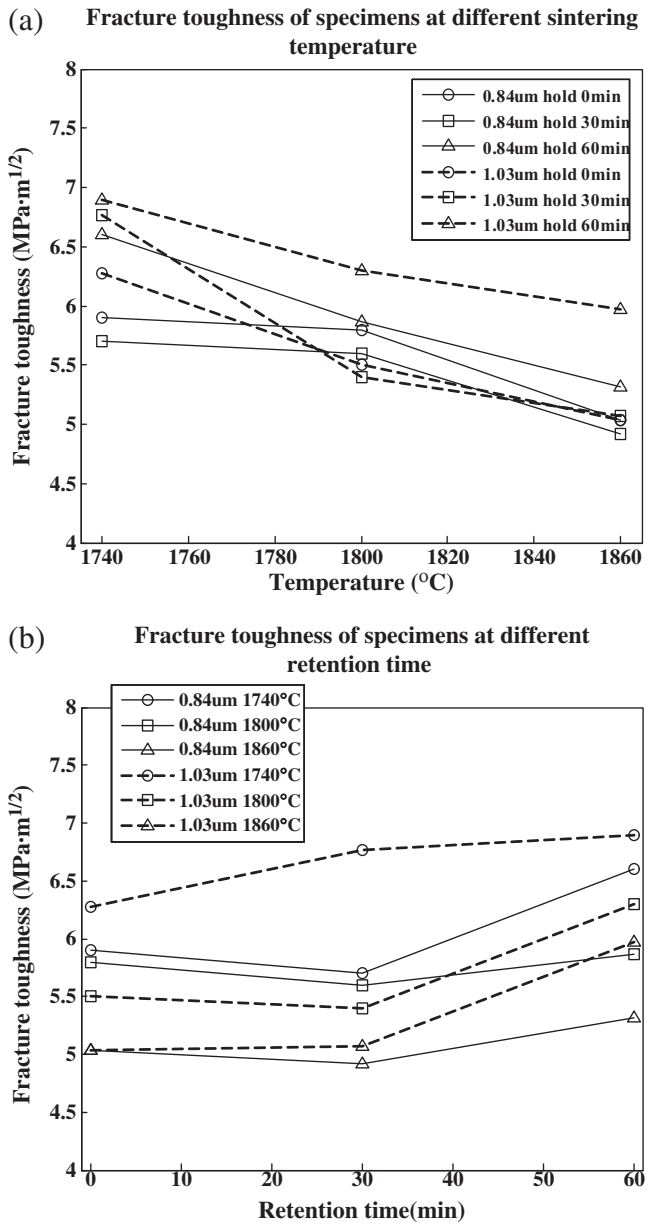

Fig. 16. Fracture toughness of specimens produced under different sintering temperatures and retention time. (a) The micro-hardness increases and the fracture toughness decreases with the increasing temperature. (b) The fracture toughness increases and the micro-hardness decreases with increasing temperature.

particles and sub-micron structure increases. Conglomeration of ultra-fine particles hampers the filling of interstitial sites while compacting of the powders produced specimens with a porous microstructure. Fig. 21 shows the amount of ultra-fine particles for the three types of powders. The concentrations of ultra-fine particles for 1.03 μm, 0.84 μm and 0.63 μm powders are 7.936%, 8.717% and 31.126% respectively. For specimens made from a 0.63 μm powder the conglomeration effect is the most severe as a result of the presence of highest percentage of ultra-fine particles, hence the softest and least dense materials are produced. Specimens with the highest micro-hardness and density are made from a 1.03 μm powder in which the concentration of ultra-fine particles is the lowest.

3.8. Comparison with other alloys

Empirical data from the literature on sintered tungsten carbides are listed as a comparison with the result of this study [16–18]. Table 2

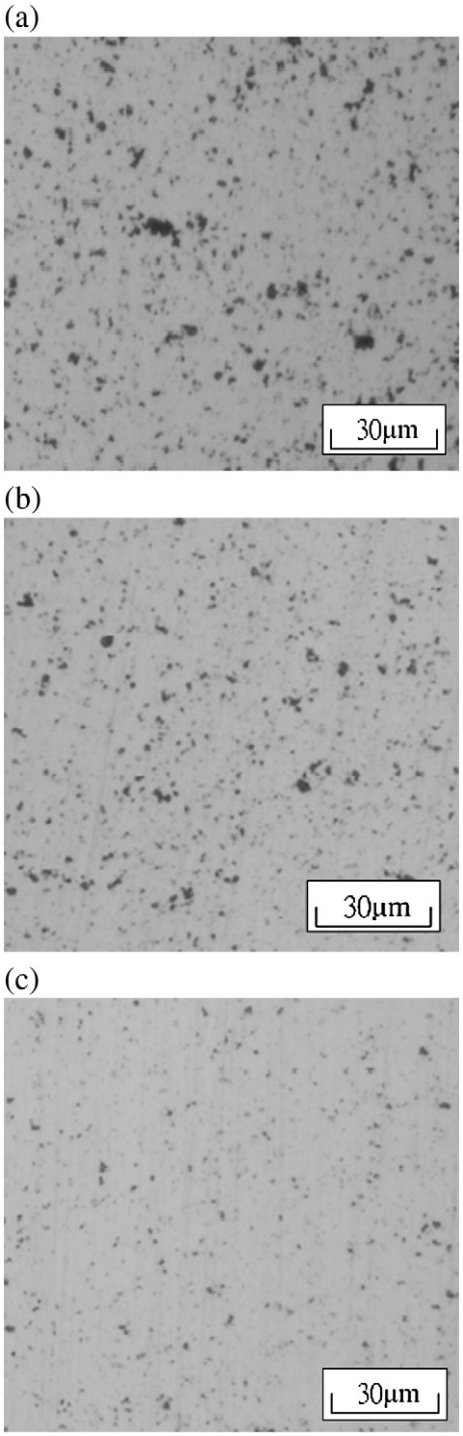

Fig. 17. OM micrographs of the samples made from a 1.03 μm powder with 60 min retention at different sintering temperature:(a)1740 °C(R.D.:91.5%, Hv:1449 kgf/mm^2, 6.9 Mpa m$^{1/2}$), (b) 1800 °C(R.D.:93.4%, Hv:1618 kgf/mm^2, 6.3 Mpa m$^{1/2}$) and (c) 1860 °C. (R.D.:95.1%, Hv:1718 kgf/mm^2, 5.97 Mpa m$^{1/2}$). The porosity decreases and the relative density and hardness increases with the increasing temperature.

lists the properties of various sintered tungsten carbides made from powders with different particle sizes; A1 is the data for binderless pure tungsten carbide in this study, while A2 and A3 are binderless pure tungsten carbide data from other researchers, with A4 through to A8 being the results for tungsten carbides with metallic binders.

The Table shows that the micro-hardness of binderless pure tungsten carbides is higher than that of tungsten carbides with binders. However, special sintering schemes are used in the Plasma

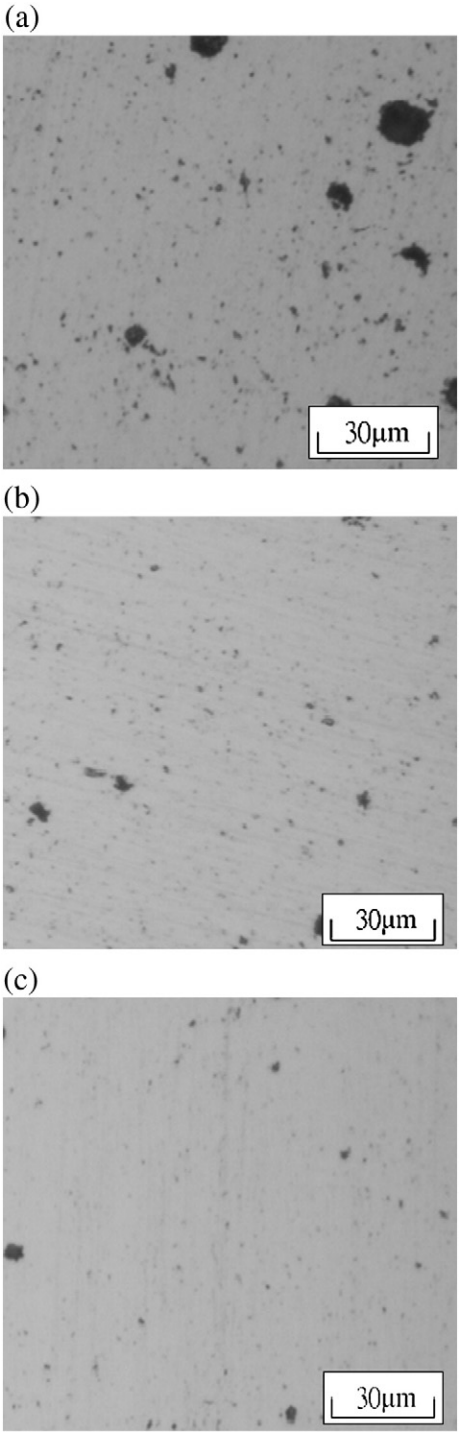

Fig. 18. OM micrographs of the samples made from mean powder size of 0.84 μm at a sintering temperature of 1860 °C with different retention time: (a) 0 min. (R.D.:87.9%, Hv:1349 kgf/mm^2, 5.04 Mpa m$^{1/2}$), b) 30 min. (R.D.:89.9%, Hv:1535 kgf/mm^2, 4.92 Mpa m$^{1/2}$) and (c) 60 min. (R.D.:90.3%, Hv:1569 kgf/mm^2, 5.32 Mpa m$^{1/2}$). The porosity decreases and the density and hardness increases with the increasing retention time.

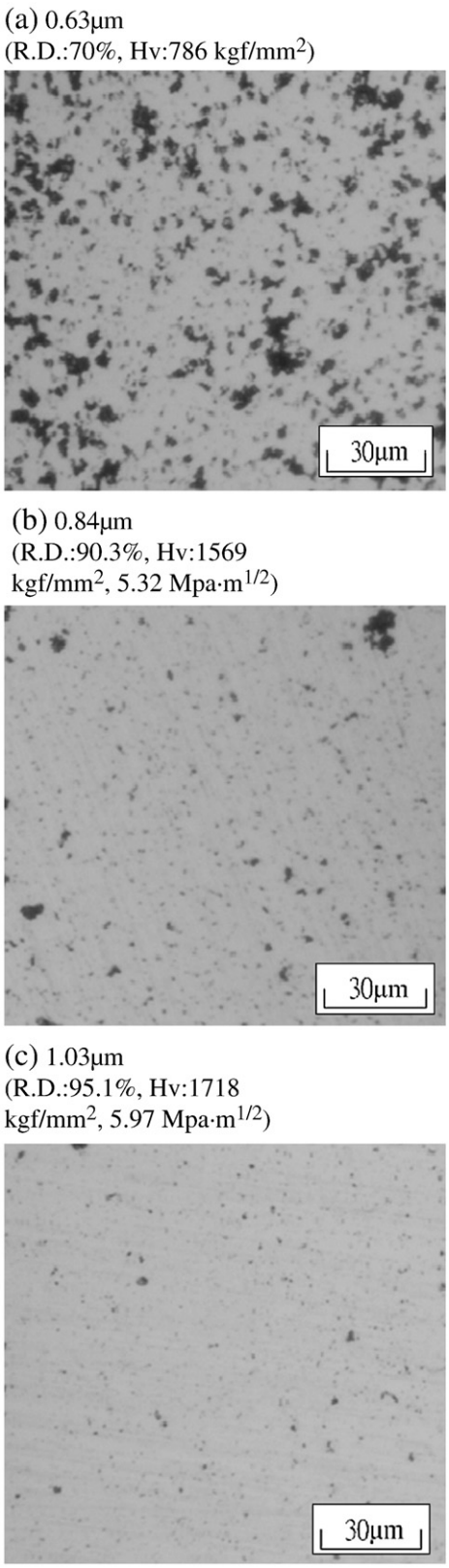

Fig. 19. OM micrographs of the samples made from WC powders with different mean particle size at a sintering temperature of 1860 °C with 60 min retention: (a) 0.63 μm (R.D.:70%, Hv:786 kgf/mm^2), (b) 0.84 μm (R.D.:90.3%, Hv:1569 kgf/mm^2, 5.32 Mpa m$^{1/2}$) and (c) 1.03 μm (R.D.:95.1%, Hv:1718 kgf/mm^2, 5.97 Mpa m$^{1/2}$). Large amount of pores are formed on the specimens because the trapped air cannot be eliminated or filled.

Pressure Compaction (A2) [16] and the High Frequency Induction Heating Sintering (A3 and A5) [17] processes to achieve higher mechanical properties. The densities of A3 and A5 suggest that Spark Plasma Sintering (SPS) technology greatly lowers the porosity in the sintered specimens; a relative density of 97% or higher are achieved. The A4 and A7 specimens are fabricated by using vacuum sintering process [11]. A low micro-hardness of 800 kgf/mm^2 is obtained for cobalt concentrations lower than 0.25%; however, for cobalt

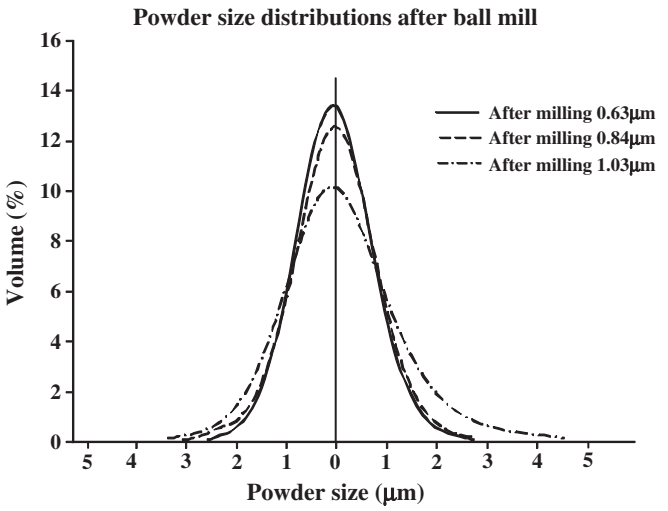

Fig. 20. Particle size distributions of the powders after 24 h ball milling. The powders with a wider distribution of particle sizes produce harder and denser samples.

concentrations higher than 1%, a hardness of 1760 kgf/mm^2 can be obtained. The results indicate that the mechanical properties for specimens produced by using vacuum sintering process are comparable with samples prepared in this study. The advanced sintering techniques such as Plasma Pressure Compaction or High Frequency Induction Heating Sintering are superior to the traditional processes in producing materials with higher density and better mechanical properties because of the high pressure used during consolidation and sintering process [1,19,20]. In pressure-assisted consolidation process, a relatively lower nominal stress is capable of inducing densification of the samples due to the presence of high local stress concentrations. At the early stage of sintering the contact area between particles is small while the effective stress is high; the contact stress decreases during the sintering process because of the contact area increasing as a result of diffusion bonding.

4. Conclusions

In this study, pure tungsten carbide powders with different particle sizes are ball milled for 24 h and sintered in a gas protecting sintering (GPS) furnace without pressure on specimens, at different temperatures and retention time to successfully produce binderless tungsten carbide material. The following conclusion can be drawn:

(1) Binderless tungsten carbide with good mechanical properties was fabricated by using GPS sintering under a set of reliable process parameters.
(2) The crystal structure analyses using XRD and EDS revealed that the substrate of the material is purely WC, without brittle W_2C or other impurity phases.
(3) The optimized set of sintering parameters is a particle diameter of 1.03 μm, a sintering temperature of 1860 °C and a retention time of 60 min; the density of the product is 95.1%, and the Vickers micro-hardness and fracture toughness of the material are 1718 kgf/mm^2 and 5.97 Mpa m$^{1/2}$ respectively.
(4) The width of particles size distribution after ball milling has a significant effect on the density and hardness of the sintered material; the width of particles size distribution is dependent on the original particle size.
(5) Ultra-fine particles increase the chance of conglomeration and sub-micron structures. For a 0.63 μm powder the concentration of ultra-fine particles (particles with diameter lower than 0.5 μm) is 31.126% which is the highest among the three types of powders. The conglomeration of ultra-fine particles hinders the filling of porosities during sintering and lowers the density and hardness of the material.

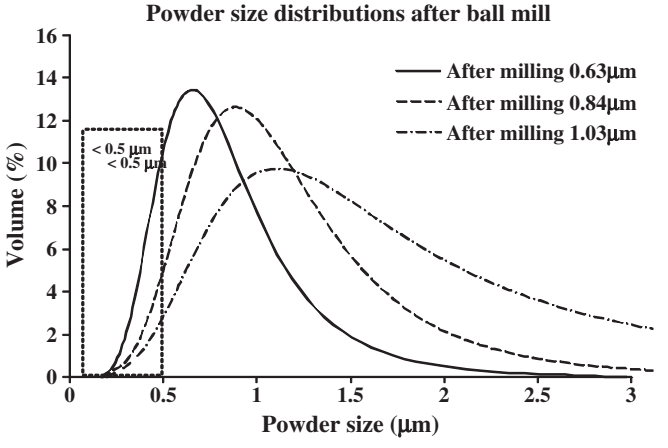

Fig. 21. Particle size distributions of the powders after 24 h ball milling showing particles with diameters less than 0.5 μm. The concentrations of particles less than 0.5 μm in diameters for 1.03, 0.84 and 0.63 μm powders are 7.936%, 8.717% and 31.126% respectively.

Table 2
Comparison of binderless tungsten carbide in this study with that in other literatures.

Number	Specimens	Relative density(%)	Hv (kgf/mm^2)	K_{IC} (MPa m$^{1/2}$)	Process[a]	Ref.
A1	$WC_{1.03\mu m}$	95.1	1718	5.97	GPS	
A2	$WC_{1.2\mu m}$	–	1950	8.2	P^2C	[16]
A3	$WC_{0.36\mu m}$	97.6	2480	6.6	HFIHS	[17]
A4	$WC_{0.7\ \mu m}$–0.25Co	91.2	<800	–	VS	[11]
A5	$WC_{0.7\ \mu m}$–1Co	97.3	1760	–	VS	[11]
A6	$WC_{0.38\ \mu m}$–10Co	98.9	1756	11.6	HFIHS	[17]
A7	P10	–	1690	8.28	GPS	[18]

[a] GPS: Gas protected sintering; P^2C: Plasma pressure compaction; HFIHS: High frequency induction heating sintering; and VS: Vacuum sintering.

References

[1] Kim HC, Shon IJ, Garay JE, Munir ZA. Consolidation and properties of binderless sub-micron tungsten carbide by field-activated sintering. Int J Refract Met Hard Mater 2004;22:257–64.
[2] Liu XQ, Lin T, Guo ZM, Cui FE, Luo JI. Consolidation of ultrafine binderless cemented carbide by spark plasma sintering. J Iron St Res Int 2007;14:82–4.
[3] Imasato S, Tokumoto K, Kitada T, Sakaguchi S. Properties of ultra-fine grain binderless cemented carbide 'RCCFN'. Int J Refract Met Hard Mater 1995;13:305–12.
[4] Bhaumik SK, Upadhyaya GS, Vaidya ML. Properties and microstructure of WC–TiC–Co and WC–TiC–Mo_2C–Co(Ni) cemented carbide. Int J Refract Met Hard Mater 1991;16:417–22.
[5] Srivatsan TS, Woods R, Petraroli M, Sudarshan TS. An investigation of the influence of powder particle size on microstructure and hardness of bulk samples of tungsten carbide. Powder Technol 2002;122:54–6.
[6] Zhu T, Manthiram A. Influence of processing parameters on the formation of WC–Co nanocomposite powder using a polymer as carbon source. Composites 1996;45:60–5.
[7] Xueming MA, Gang JI, Ling Z, Yuanda D. Structure and properties of bulk nanostructured WC–CO alloy by mechanical alloying. J Alloy Comp 1998;264:267–70.
[8] Sommer M, Schubert WD, Zobetz EA, Warbichler P. On the formation of very large WC crystals during sintering of ultrafine WC–Co alloys. Int J Refract Met Hard Mater 2002;20:41–50.
[9] Anstis GR, Chantikul P, Lawn BR, Marshall DB. A critical evaluation of indentation techniques for measuring fracture toughness: I, direct crack measurements. J Amer Ceram Soc 1981;64:533–8.
[10] Zhao J, Holland T, Unuvar C, Munir ZA. Sparking plasma sintering of nanometric tungsten carbide. Int J Refract Met Hard Mater 2008;27:130–9.
[11] Li T, Li Q, Fuh JYH, Yu PC, Wu CC. Effects of lower cobalt binder concentrations in sintering of tungsten carbide. Mater Sci Eng 2006;A430:113–9.
[12] Chen KS. Introduction to powder metallurgy. Taiwan: Chuan Hwa; 1995 (in Chinese).

[13] Wang JM. Powder metallurgy technology. Taiwan: Powder Metall Associ ROC; 1994 (in Chinese).
[14] Huang B, Chen LD, Bai SQ. Bulk ultrafine binderless WC prepared by spark plasma sintering. Scr Mater 2006;54:441–5.
[15] McCandlish LT, Kear BK, Kim BK. Chemical processing of nanophase WC–Co composite powder. J Mater Technol 1990;19:953–7.
[16] Staia MH, Torres IJ, Castillo C, Sudarshan TS, Lesage J, Chicot D. Tribological study of WC produced by plasma pressure compaction. Int J Refract Met Hard Mater 2006;24:183–8.
[17] Kim HC, Shon IJ, Yoon JK, Doh JM. Consolidation of ultra fine WC and WC–Co hard materials by pulsed current activated sintering and its mechanical properties. Int J Refract Met Hard Mater 2005;25:46–52.
[18] Lin YY. A study of fabrication and cutting of tungsten carbide materials. N Chin-Yi Univers Techn, Master thesis, 2005.
[19] Cha SI, Hong SH. Microstructures of binderless tungsten carbides sintered by spark plasma sintering process. Mater Sci Eng 2003;A356:381–9.
[20] Shon IJ, Kim BR, Doh JM, Yoon JK, Woo KD. Properties and rapid consolidation of ultra-hard tungsten carbide. J Alloy Comp 2010;489:L4–8.